



# Synthesis of copper (II) complexes incorporating *N,N*-dimethyl-*N'*-benzylethylenediamine and NCX (X = O, S and Se) ligands: A combined crystallographic, spectroscopic and DFT study

Hamid Golchoubian\*, Sara Koohzad, Maedeh Ramzani, Davood Farmanzadeh

Department of Chemistry, University of Mazandaran, Babolsar 47416-95447, Iran

## ARTICLE INFO

### Article history:

Received 24 October 2012

Accepted 4 December 2012

Available online 27 December 2012

### Keywords:

Copper (II), DFT study

Linkage isomer

X-ray structure

Pseudohalide ligand

Solvatochromism

## ABSTRACT

Three copper (II) complexes of type  $[\text{Cu}(\text{L})_2(\text{NCX})]\text{ClO}_4$ , **1–3**, (L = *N,N*-dimethyl-*N'*-benzyl-1,2-diaminoethane and X = O, S and Se) were synthesized and characterized on the basis of microanalytical, spectroscopic and molar conductance. An X-ray diffraction study of  $[\text{Cu}(\text{L})_2(\text{NCO})]\text{ClO}_4$  (**1**) reveals that the copper (II) center located in a distorted square pyramidal environment through coordination of four amine N atoms and a N atom of the terminal  $\text{NCO}^-$ . Density functional theory (DFT) calculations were performed to understand the linkage isomerism of  $\text{NCX}^-$  ligand from a theoretical point of view, to study the electronic structure of the complexes and the relative stabilities of the Cu–NCX/Cu–XCN isomers. DFT computational results buttressed the experimental observations indicating that the Cu–NCX isomer is more stable than Cu–XCN linkage isomer. Complexes **1** and **2** exhibit solvatochromism as evidenced from visible study in different solvents.

© 2012 Elsevier Ltd. All rights reserved.

## 1. Introduction

Linkage isomerism is a type of phenomenon that is characteristic of transition metal complexes, where the ambidentate ligands are capable binding through different binding sites. A large verity of linkage isomers involving ligands such as  $\text{NCO}^-$ ,  $\text{NCS}^-$ ,  $\text{NCSe}^-$ ,  $\text{CN}^-$ ,  $\text{NO}^-$ ,  $\text{NO}_2^-$ ,  $\text{SO}_3^-$ , and so forth were reported in recent years. The coordination compounds of these ligands involve mostly in mononuclear form. Among the ambidentate ligands the  $\text{NCX}^-$  (X = O, S, Se) ion has been the most well known and is able to coordinate through either N or X end. Indeed, the  $\text{NCX}^-$  ion has the capabilities of N- and X-coordinations as a unidentate ligand, and of bridging bonding. So far, several studies on the linkage isomerism of thiocyanate and isothiocyanate have been conducted for the third (Pt(II) [1,2], Re(V) [3–5] Ru(III) [6]), second (Pd(II) [7], Ru(III) [8]) and first row (cobalt (III) [9], Cu(II) [10]) transition metal ions but less attention has been focused on  $\text{NCO}^-$  and  $\text{NCSe}^-$  linkage isomers. Normally, the softness or hardness of metal ions determines the coordination mode of the  $\text{NCX}^-$  ion. The S or Se-bonding has been generally associated to the softness of the metal ion, but this not provide a sufficient condition, since this depends on the nature of the ancillary coordinated ligands as well as steric factor. Copper (II) ion is a borderline Lewis acid and it is expected to bind through the two sides of the X and N of the  $\text{NCX}^-$ , but higher

tendency to coordinate to the nitrogen [11–14]. Prettiness of copper ions in these compounds is mainly due to the magnetic properties of copper (II) ion, photoluminescence, mixed-valence oxidation state, structural features, color, conductivity and biological relevance concerning the dinuclear site in cytochrome oxidases and associated model compounds [15]. Another attractive aspect of copper (II) complexes is the coordination geometry about the metal ion. Copper (II) can exist in coordination numbers four, five and six. In five-coordinate, copper (II) ion usually demonstrate intermediate stereochemical environment ranging between square pyramidal and trigonal bipyramidal, depending on the nature of the co-ligands [16,17].

Recently, theoretical calculations using the DFT formalism are becoming very popular in order to understand detailed electronic structures of complicated coordination compounds from a microscopic viewpoint. In particular, we are interested in applying the DFT calculations for understanding and predicting linkage isomerism of various systems. Several DFT calculations on linkage isomerism of ruthenium complexes have previously been performed [18–23]. For example, Stener and Calligaris calculated the relative energy of O-bonded and S-bonded isomers of  $[\text{Ru}^{\text{II}}(\text{NH}_3)_5(\text{dmsO})]^{2+}$  [24], where the S-bonded isomer was found to be slightly more stable than the O-bonded isomer by  $13 \text{ kJ mol}^{-1}$  using the gas-phase model. Ghosh et al. performed the DFT calculations of linkage isomers of  $[\text{Ru}^{\text{II}}(\text{H}_3\text{tctpy})(\text{SCN})_3]^-$  ( $\text{H}_3\text{tctpy} = 4,4',4''\text{-tricarboxy-2,2':6,2''-terpyridine}$ ) in order to assign the experimentally-observed electronic absorption spectra [20].

\* Corresponding author. Tel./fax: +98 1125342350.

E-mail address: [h.golchoubian@umz.ac.ir](mailto:h.golchoubian@umz.ac.ir) (H. Golchoubian).

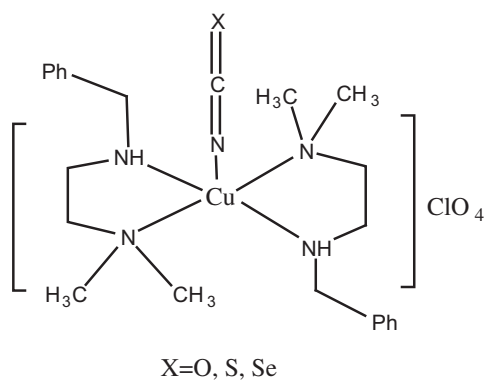


Fig. 1. The complexes used in this study.

In order to get further insight into the different stability of  $\text{NCX}^-$  linkage isomers and into the nature of metal to X bond in case of “borderline” metal like copper (II), we have undertaken a DFT study on the three new copper (II) complexes  $[\text{Cu}(\text{L})_2(\text{NCX})]\text{ClO}_4$ , where L = *N,N*-dimethyl,*N'*-benzyl-1,2-diaminoethane and X = O, S and Se as shown in Fig. 1. The aim of this study is to investigate the bonding mode of the  $\text{NCX}^-$  in the most stable isomer.

## 2. Experimental

### 2.1. Materials and measurements

*N,N*-dimethyl,*N'*-benzyl-ethylenediamine was prepared according to our published procedure [25]. All solvents were spectral-grade and all other reagents were used as received. All the samples were dried to constant weight under a high vacuum prior to analysis. *Caution! Perchlorate salts are potentially explosive and should be handled with appropriate care.*

Conductance measurements were made at 25 °C with a Jenway 400 conductance meter on  $1.00 \times 10^{-3}$  M samples in selective solvents. Infrared spectra (potassium bromide disk) were recorded using a Bruker FT-IR instrument. The electronic absorption spectra were measured using a Braic2100 model UV–Vis spectrophotometer. Elemental analyses were performed on a LECO 600 CHN elemental analyzer. Absolute metal percentages were determined by a Varian-spectra A-30/40 atomic absorption-flame spectrometer. The following solvents were used for solvatochromic study: dichloromethane (DCM), benzonitrile (BN), acetone (Ac), dimethylformamide (DMF), dimethylsulfoxide (DMSO) and hexamethylphosphorotriamide (HMPA).

### 2.2. Synthesis

#### 2.2.1. Preparation of $[\text{Cu}(\text{L})_2(\text{NCO})]\text{ClO}_4$ (1)

A typical procedure is as follow: to the solution of the diamine ligand (0.356 g, 2 mmol) and NaNCO (0.065 g, 1 mmol) in ethanol (30 mL) were slowly added  $\text{Cu}(\text{ClO}_4)_2 \cdot 6\text{H}_2\text{O}$  (0.37 g, 1 mmol) in ethanol (10 mL). The resultant mixture was stirred for 1 h at room temperature. The desired compound precipitated from the reaction mixture as a blue solid. The crude compound was recrystallized from diffusion of diethyl ether into acetonitrile solution. The typical yield was 41%. Selected IR data ( $\nu/\text{cm}^{-1}$  KBr disk): 3257 (s, N–H str.), 2210 (s,  $\text{OCN}^-$  str.), 1455 (m,  $\text{CH}_2$ –Ph str.), 1097 (s,  $\text{ClO}_4$  str.), 808, (w, C–N str.), 622 (m,  $\text{ClO}_4$  bend). *Anal. Calc.* For  $\text{C}_{23}\text{H}_{36}\text{CuN}_5\text{ClO}_5$  (MW = 561.56 g mol $^{-1}$ ): C, 49.21; H, 6.52; N, 12.53; Cu, 11.32. Found: C, 49.31; H, 6.66; N, 12.51; Cu, 11.22%.

#### 2.2.2. Preparation of $[\text{Cu}(\text{L})_2(\text{NCS})]\text{ClO}_4$ (2)

This complex was prepared by a similar method used for  $[\text{Cu}(\text{L})_2(\text{NCO})]\text{ClO}_4$  except that NaNCS was used in place of NaNCO. The compound was obtained as a green solid with typical yield of 53%. Selected IR data ( $\nu/\text{cm}^{-1}$  using KBr): 3254 (s, N–H str.), 2077 (s,  $\text{SCN}^-$  str.), 1455 (m,  $\text{CH}_2$ –Ph str.), 1088 (s,  $\text{ClO}_4$  str.), 811, (w, C–N str.), 622 (m,  $\text{ClO}_4$  bend). *Anal. Calc.* for  $\text{C}_{23}\text{H}_{36}\text{CuN}_5\text{ClO}_4\text{S}$  (MW = 577.63 g mol $^{-1}$ ): C, 47.83; H, 6.28; N, 12.12; Cu, 11.00. Found: C, 47.85; H, 6.39; N, 12.07; Cu, 11.08%.

#### 2.2.3. Preparation of $[\text{Cu}(\text{L})_2(\text{NCSe})]\text{ClO}_4$ (3)

This compound was synthesized with the similar procedure used for  $[\text{Cu}(\text{L})_2(\text{NCO})]\text{ClO}_4$  except that NaNCSe was used instead of NaNCO. The compound was obtained as an olive green solid with typical yield of 46%. Selected IR data ( $\nu/\text{cm}^{-1}$  using KBr): 3248 (s, N–H str.), 2126 (s,  $\text{SeCN}^-$  str.), 1455 (m,  $\text{CH}_2$ –Ph str.), 1087 (s,  $\text{ClO}_4$  str.), 813, (w, C–N str.), 626 (m,  $\text{ClO}_4$  bend). *Anal. Calc.* for  $\text{C}_{23}\text{H}_{36}\text{CuN}_5\text{ClO}_4\text{Se}$  (MW = 624.52 g mol $^{-1}$ ): C, 44.23; H, 5.81; N, 11.21; Cu, 10.18. Found: C, 44.54; H, 5.30; N, 10.98; Cu, 11.29%.

### 2.3. X-ray structure determination

A suitable single crystal of **1** was glued on the tip of a glass fiber. The X-ray data were collected at room temperature by  $\omega$ -scans on STOE IPDS-II diffractometer with graphite-monochromated Mo  $K\alpha$  radiation ( $\lambda = 0.71073 \text{ \AA}$ ). Data reduction, including the absorption correction, was performed with the X-Area Software software package [26]. Solution, refinement and analysis of the structure were performed by using SHELXTL programs [27,28]. The structure was solved by direct method (SIR92) [29] and refined by the full-matrix least-squares method based on  $F^2$  against all reflections [30]. Geometrical calculations were carried out with PLATON [31] and the figures were made by the use of the Diamond [32] and MERCURY [33] programs. The complete conditions of data collection and structure refinements are given in Table 1. The hydrogen atoms of NH groups were found in difference Fourier synthesis. The H(C) atom positions were calculated. All hydrogen atoms were refined in isotropic approximation in riding model with the Uiso(H) parameters equal to 1.2 Ueq(Ci), for methyl groups equal to 1.5 Ueq(Cii), where U(Ci) and U(Cii) are respectively the equivalent thermal parameters of the carbon atoms to which corresponding H atoms are bonded. The weighted *R*-factor *wR* and goodness of fit *S* are based on  $F^2$ , conventional *R*-factors *R* are based on *F*, with *F* set to zero for negative  $F^2$ . The threshold expression of  $F^2 > 2\sigma(F^2)$  is used only for calculating *R*-factors(gt) etc., and is not relevant to the choice of reflections for refinement. The atomic coordinates correspond to the absolute structure of the molecule in the crystal.

### 2.4. Computational method

Calculations were carried out using GAUSSIAN09 package program [34]. The X-ray crystallographic structure for  $[\text{Cu}(\text{L})_2(\text{NCO})]\text{ClO}_4$  was used as a starting coordinate to generate  $[\text{Cu}(\text{L})_2(\text{NCX})]\text{ClO}_4$  (X = NCS, NCSe) geometries. In the computational model, the perchlorate anion was ignored and the monocationic complex was taken into account. The optimized geometries were verified by performing a frequency calculation. The vibrations in the calculated vibrational spectrum were real, thus the optimized geometries correspond to true energy minimum. Density functional theory (DFT) was carried out on the gas phase of complexes using the Beck three parameters hybrid exchange [35] and the Lee–Yang–Parr correlation hybrid functional [36] (B3LYP) and mixed basis set, LANL2DZ basis set including effective core potential (ECP) of Hay and Wadt [37–39] used for Cu and 6-31+G(d,p) for the others(GEN).

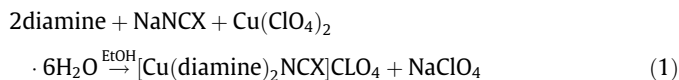
**Table 1**  
Crystal data and structure refinement of complex **1**.

Empirical formula	C <sub>23</sub> H <sub>36</sub> CuN <sub>5</sub> O·ClO <sub>4</sub>
Formula weight	561.57
Color	needle, blue
T (K)	295(2)
λ (Å)	0.71073
Crystal system	monoclinic
Space group	P2 <sub>1</sub>
Crystal size (mm)	0.20 × 0.11 × 0.09
Unit cell dimensions	
a (Å)	9.961(2)
b (Å)	9.2187 (18)
c (Å)	14.583 (3)
β (°)	94.92 (3)
V (Å <sup>3</sup> )	1334.2 (5)
Z	2
Calculated density	1.398 Mg/m <sup>3</sup>
Absorption coefficient	0.96 mm <sup>-1</sup>
F(000)	590
θ (°)	2.09–25.00
Index ranges	−11 ≤ h ≤ 11 −10 ≤ k ≤ 10 −17 ≤ l ≤ 17
μ (mm <sup>-1</sup> )	0.96
Reflections collected/unique	10493/2659 [R(int) = 0.089]
Completeness to θ = 30.10	99.5%
Absorption correction	multi-scan
Refinement method	full-matrix least-square on F <sup>2a</sup>
Data/restraints/parameters	4324/1/30
Final R indices <sup>a</sup> [I > 2σ(I)] <sup>b</sup>	R <sub>1</sub> = 0.0860, wR <sub>2</sub> = 0.0861
Goodness-of-fit (GOF) on F <sup>2c</sup>	1.006
R indices (all data)	R <sub>1</sub> = 0.1483, wR <sub>2</sub> = 0.0753
Largest difference in peak and hole (e Å <sup>-3</sup> )	0.802 and −0.478
Flack parameter	0.01(5)

<sup>a</sup>  $R = \sum(|F_o| - |F_c|) / \sum|F_o|$ .<sup>b</sup>  $wR = \{[\sum(F_o^2 - F_c^2)^2] / \sum w(F_o^2)^2\}^{1/2}$ .<sup>c</sup>  $S = \sum[w(F_o^2 - F_c^2)^2 / (N_{obs} - N_{param})]$ .

### 3. Results and discussion

All complexes were synthesized by mixing of diamine, Cu(ClO<sub>4</sub>)<sub>2</sub>·6H<sub>2</sub>O and NaNCX with the molar ratios of 2:1:1, respectively in ethanol as shown in Eq. (1).



The complex, **3** was only partially soluble in dimethyl sulfoxide and was nearly insoluble in all other solvents investigated. Thus, thorough characterization and establishment of the purity of this compound were hindered by its poor solubility. Analytical data, molar conductivity, IR spectra and X-ray crystallography indicated formation of the desired copper (II) complexes.

#### 3.1. IR spectra

In the IR spectra of compounds **1–3** several bands appear in the region 600–3500 cm<sup>-1</sup> that are also observed, although with minor shifts, in the spectra of the free ligands. In addition, certain absorption bands that are characteristic of the NCX<sup>-</sup> ions exist in the IR spectra of the complexes. Appearance of the perchlorate bands at around 1100 and 630 cm<sup>-1</sup> in complexes are indicative of the ionic nature of the complexes. The intense absorption band in the region around 2100 cm<sup>-1</sup> in the complexes is assigned to the NCX<sup>-</sup> vibrational mode in which shifted to the lower wave numbers in compared to the free NCX<sup>-</sup> because of coordination to the copper center [40,41]. Dependence on coordination of the diamine chelate is also exhibited by an intense and narrow band occurring at 3290 ± 10 cm<sup>-1</sup> which is associated with N–H vibration and is

observed at around 3350 cm<sup>-1</sup> and broader in the free diamine ligands. As the lone pair of electrons of the donor nitrogen atoms become involved in the metal–ligand bond, the transfer of the electron density to the metal and the subsequent polarization of the ligands involves electron depopulation of the N–H bond that culminates in a shift to lower frequencies. The vibrational bands around 1040 cm<sup>-1</sup> are corresponded to the stretching vibration of C–N bond and the bands around 1450 cm<sup>-1</sup> are associated to the scissoring vibration of –CH<sub>2</sub>– phenyl groups [42]. The strong bands around 1365 cm<sup>-1</sup> are associated to the bending vibrations of CH<sub>3</sub> groups. The existence of an intense and sharp band occurring at 2210 cm<sup>-1</sup> together with a band of weak intensity at 808 cm<sup>-1</sup> attributed to the stretching frequency of ν<sub>CO</sub> that confirms the coordination of NCO ligand through N-atom to the Cu(II) ion in complex **1** [43–45]. This coordination mode was confirmed by the X-ray analysis. The presence of NCS<sup>-</sup> group in complex **2** and coordination through the nitrogen atom to the copper (II) ion is declared by an intense band at 2077 cm<sup>-1</sup> which is attributed to the symmetric ν<sub>NCS</sub> stretching vibration mode [46,47]. This band is consistent with N-bonded thiocyanato ligand, a fact that can be further substantiated from an absorption band at 811 (medium) cm<sup>-1</sup>, which is attributed to the stretching frequency of ν<sub>CS</sub> for N-bonded thiocyanato ligand. The infrared spectrum of the isose-lenocyanato, complex **3** shows a sharp band at 2126 cm<sup>-1</sup> that is assigned to the stretching frequency of ν<sub>NCS<sub>e</sub></sub>. This assignment is combined with a weak band at 813 cm<sup>-1</sup> that account for the stretching frequency of ν<sub>CS<sub>e</sub></sub> and indicated the monodentate N-coordination of the NCS<sub>e</sub> ligand to the Cu(II) ion [48].

The calculated (non-scaled) vibrational spectra of compounds **1–3** stay in good agreement with the experimental data, as

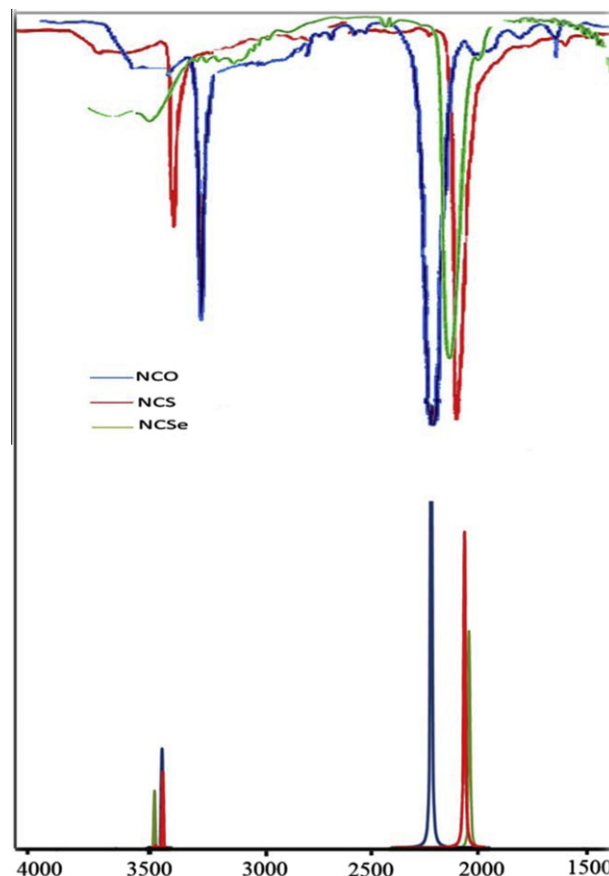


**Fig. 2.** Comparison of the experimental IR spectra (–NCX and N–H vibrations) of solid [Cu(L)<sub>2</sub>(NCO)]ClO<sub>4</sub>, [Cu(L)<sub>2</sub>(NCS)]ClO<sub>4</sub> and [Cu(L)<sub>2</sub>(NCS<sub>e</sub>)]ClO<sub>4</sub> on KBr pellets (top) with theoretical results (bottom) in the 1700–4000 cm<sup>-1</sup> frequency range.

**Table 2**

Molar conductivity data ( $\Lambda_m$ ) of the complexes **1** and **2** ( $\Omega^{-1} \text{ cm}^2 \text{ mol}^{-1}$ , at 25 °C) in different solvents.

Complex	NM	NB	ACN	AC	EtOH	MeOH	DMF
<b>1</b>	74.2	17.5	134.8	107.6	36.0	76.2	60.0
<b>2</b>	70.7	16.3	149.0	114.6	21.0	57.5	59.5
1:1 Electrolyte	95–75	30–20	160–120	140–100	45–35	115–80	90–65

presented in Fig 2. The calculated  $\nu_{\text{CN}}$  strong absorptions occur at 2214, 2060 and 2010  $\text{cm}^{-1}$  for complex **1**, **2** and **3**, respectively. These values are in agreement with the corresponding experimental ones by  $\sim 1\%$  error. Similarly, the calculated absorptions due to  $\nu_{\text{N-H}}$ ,  $\nu_{\text{C=C}}$  modes of the diamine ligand appearing at 3450 and 3459  $\text{cm}^{-1}$ , fall in the experimental ranges.

### 3.2. Conductometric data

Table 2 shows the molar conductivity values of complexes **1** and **2** and the standard values for 1:1 electrolytes in different solvents [49]. The results exhibited that the complexes are 1:1 electrolyte in all solvents investigated.

### 3.3. X-ray structure

An ORTEP view of the cationic part of complex **1** is depicted in Fig. 3 together with the numbering scheme. Selected bond distances and angles are presented in Table 3. The compound crystallizes in the monoclinic space group  $P2_1$ . The geometry about the copper can be regarded as a distorted square-pyramid with the  $\text{N}_5$  donor atoms. The geometric discrimination parameter  $\tau$  [50] between square-pyramid ( $\tau = 0$ ) and trigonal-bipyramid ( $\tau = 1$ ) is 0.28. The two five-membered rings of the diamine chelate are almost perpendicular to each other in around of the copper center ( $79.69^\circ$ ). The cyanate ligand is located in the base and the nitrogen atom of the diamine chelate, N(5) is at apex. The  $\text{OCN}^-$  group is almost linear, with N–C–O angles of  $175.0(2)$ . The  $\text{NCO}^-$  group in the equatorial plane forms Cu–N–C angle of  $164.4(1)$ . The copper (II) ion is displaced by  $0.245(4)$  Å from the basal least square plane toward the N(5) atom. The mean bite angle of N–Cu–N of the diamine ligand is  $82.4(5)^\circ$  and close to the related values of the analogous copper (II) complexes [51–53]. The mean basal Cu–N distance of the diamine chelate is  $2.084(9)$  Å but axial Cu–N(5) (diamine) bond is elongated [ $2.326(7)$  Å] owing to Jahn–Teller effect for  $d^9$  electronic configuration. The asymmetric nitrogen atoms

N(3) and N(4) have *R* and *S* configurations, respectively in the Fig. 3; the benzyl substituent on the amine chelates are situated *cis* to each other. The packing of the structure in the unit cell is shown in Figs. 4 and 5. This arrangement shows that perchlorate, as the counter ion, has no any interaction with copper (II) center probably due to steric hindrance around the copper and is located far-off from this center. In the compound, through N(4)H $\cdots$ O(3) ( $2.493$  Å) and N(2)H $\cdots$ O(4) ( $2.554$  Å) hydrogen bonds, an 1D zigzag chain structure is found (Fig. 4), which is further linked to the neighboring one via weak contacts C(1) $\cdots$ H(21)C ( $2.883$  Å), extending to a hydrogen-bonded 2D supramolecular layer (Fig. 5).

### 3.4. Theoretical considerations

There are two linkage isomers for all three complexes as Cu–NCX and Cu–XCN. The DFT calculations were therefore performed, in order to interpret the experimental results. The X-ray structure available for the family of the complexes in this work is  $[\text{Cu}(\text{L})_2(\text{NCO})]\text{ClO}_4$ . We started by optimizing the geometry of this complex, without any symmetry constraints in order to calibrate the method. The optimized structure with labeling of the atoms is shown in Fig. 3. Consistent with the crystallographic results gathered in Table 3 geometrical parameters for complex **1** are in agreement with the experimental results (with deviations ranging from  $+0.030$  to  $-0.086$  Å for basal Cu–N bonds). The error for the axial Cu–N bond length is larger ( $+0.203$  Å). The deviation may come from the basis sets which are approximated to a certain extent or may indicate the influence of the crystal packing on the values of the experimental bond lengths because the theoretical calculations do not consider the effects of chemical environment. Unfortunately there is no way to predict the energy difference in the solid state. The relative stability of  $\text{X}^-$  and  $\text{N}^-$  isomers in the complexes has been evaluated from the difference between their total energies,  $\Delta E^{\text{N-X}} = |E^{\text{N}} - E^{\text{X}}|$ . The greater the  $\Delta E^{\text{N-X}}$  value, the greater the stability of the N-isomers. According to the present DFT calculations, the N-bonded isomers appear more stable than the X-isomers in all complexes (Table 4). Calculations show that  $\Delta E^{\text{N-X}}$  increases with the increasing of the donor power of X (Se > S > O).

In order to understand the source of the observed difference in relative energies more quantitatively, we have performed atomic charge analyses. Table 5 summarizes the results of NPA calculations for the Cu–NCX and Cu–XCN structures. This result shows the effective charge on the Cu atom significantly affects the strength of the Cu–X or Cu–N bond in coordination complexes. Taking two fragments,  $[\text{Cu}(\text{L})_2]^{2+}$  and  $\text{XCN}^-$ , as references, we can also calculate the value of the transferred charge. From Table 5,

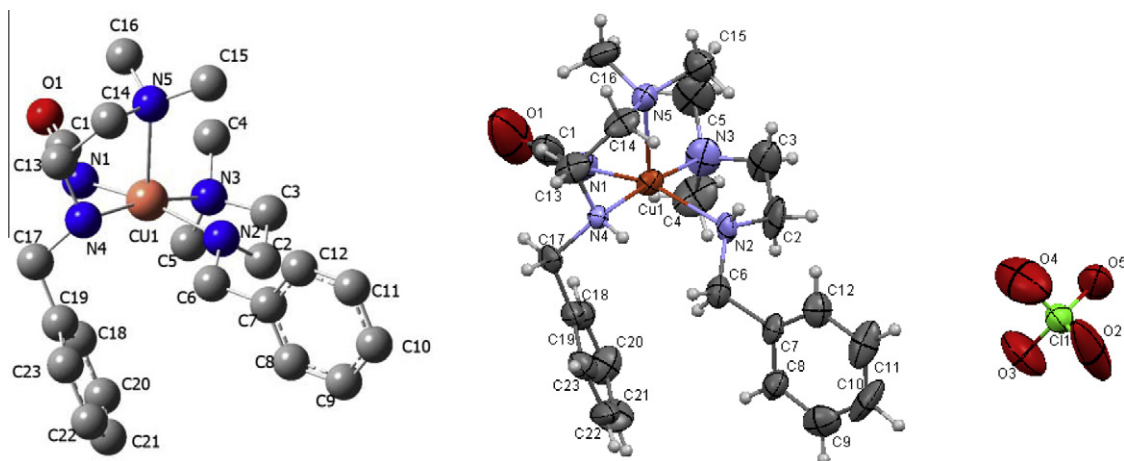
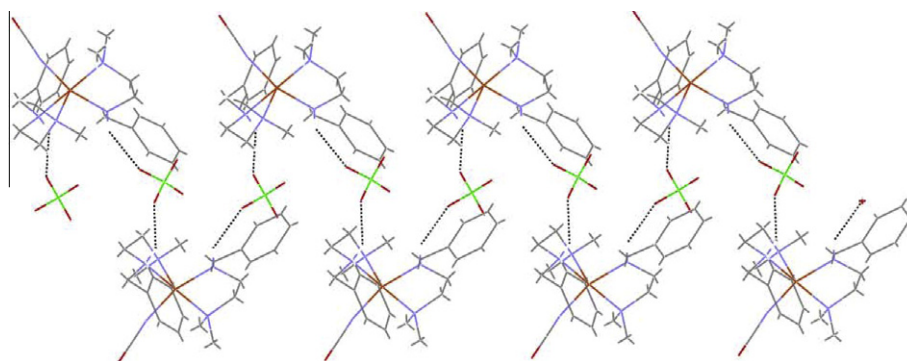
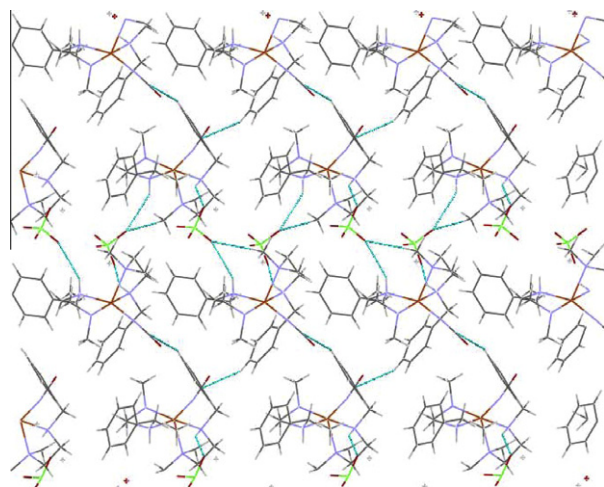


Fig. 3. ORTEP view (right) and the optimized geometry (left) of the complex **1** together with its labeling.

**Table 3**The selected experimental and optimized bond lengths (Å) and angles (°) for complex **1**.

Bond distances(Å)	Bond angles(°)				
	Experimental	Theoretical	Experimental	Theoretical	
N(1)–Cu(1)	1.934 (10)	1.964	N(4)–Cu(1)–N(3)	173.9 (4)	169.09572
N(2)–Cu(1)	2.105 (9)	2.149	N(4)–Cu(1)–N(2)	94.1 (3)	95.77873
N(3)–Cu(1)	2.077 (9)	2.163	N(3)–Cu(1)–N(2)	82.8 (4)	83.11360
N(4)–Cu(1)	2.072 (8)	2.123	N(1)–Cu(1)–N(5)	97.1 (4)	98.17514
N(5)–Cu(1)	2.326 (7)	2.528	N(4)–Cu(1)–N(5)	82.3 (3)	80.39524
C(1)–N(1)	1.119 (15)	1.213	N(5)–Cu(1)–N(3)	103.6 (4)	110.48869
C(1)–O(1)	1.207 (15)	1.215	N(2)–Cu(1)–N(5)	105.7 (3)	93.90039
Bond angles(°)			N(1)–Cu(1)–N(2)	157.1 (4)	167.8
N(1)–Cu(1)–N(4)	90.7 (4)	87.3	C(1)–N(1)–Cu(1)	165.4 (11)	144.95409
N(1)–Cu(1)–N(3)	90.2 (4)	91.6	N(1)–C(1)–O(1)	175.0 (15)	178.32873

**Fig. 4.** 1D zigzag chain structure of compound **1** along the *b*-axis with hydrogen bonds indicated by dotted lines.**Fig. 5.** 2D supramolecular architecture of compound **1** viewing down the *a*-axis with hydrogen bonds indicated by dotted lines.

the charges transferred from the  $\text{XCN}^-$  moiety to the metallic moiety are in the ranges of 0.66–0.70  $|e^-|$  and 0.53–0.70  $|e^-|$  for Cu–N and Cu–X, respectively. From charge transfer interactions we can see that the contribution of nitrogen atoms coordinating to the copper ion is much greater than that of sulfur atom.

The Cu–N bond distances in all three complexes of Cu–NCX are shorter than in their counterparts Cu–S bond lengths of Cu–SCN complexes. The differences are between 0.496–0.456 Å.

The geometries of complexes **2** and **3** were optimized in doublet state using the DFT method with the B3LYP functional in gas phase. The calculated geometric parameters of  $[\text{Cu}(\text{L})_2(\text{NCS})]^+$  and

**Table 4**Differences between total molecular energies ( $\Delta E^{\text{N-X}}$ ,  $\text{kJ mol}^{-1}$ ) for N and X bonded isomers of the complexes<sup>a</sup>.

Complexes	$E$ (kJ/mol)	$E$ (kJ/mol)	$E$ (kJ/mol)
Cu–NCO–	0.0	Cu–NCS <sup>−</sup> −847960	Cu–NCSe <sup>−</sup> −6100880
Cu–OCN	40	Cu–SCN −847910	Cu–SeCN −6100840

<sup>a</sup> The molecular energy of  $[\text{Cu}(\text{L})_2(\text{NCO})]^+$  was taken as a reference.

**Table 5**

Results of natural population analysis for Cu–NCX and Cu–XCN isomers.

	Cu	N	C	X	NCX
Cu–NCX					
X = O	0.99	−0.859	0.70	−0.54	−0.70
X = S	0.989	−0.69	0.11	−0.12	−0.70
X = Se	0.969	−0.66	0.03	−0.03	−0.66
Cu–XCN					
X = O	1.04	−0.49	0.52	−0.75	−0.70
X = S	0.85	−0.33	0.03	−0.23	−0.53
X = Se	0.80	−0.32	−0.04	−0.09	0.55

$[\text{Cu}(\text{L})_2(\text{NCSe})]^+$  are gathered in Tables 6 and 7, respectively. Their optimized structures are shown in Fig. 6. The optimized geometries for the complexes display distorted square pyramidal environments and general trends observed in the experimental data are satisfactorily reproduced in the calculations.

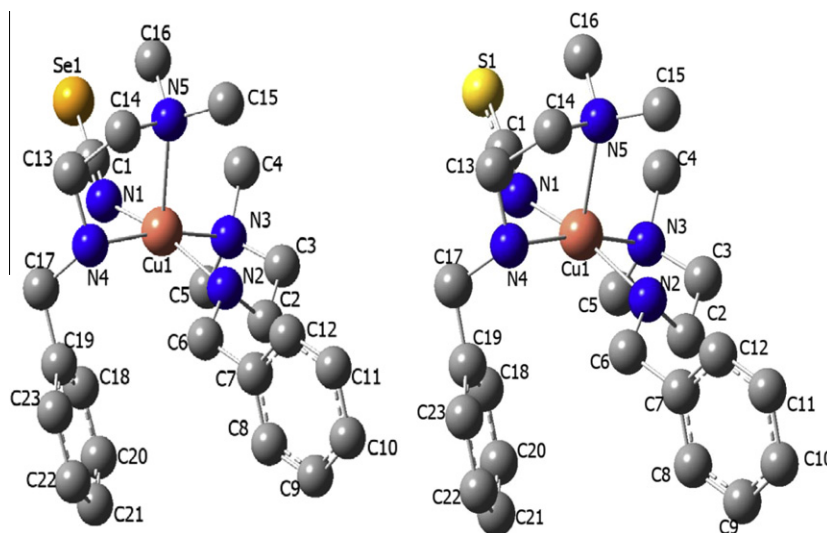
A schematic illustration of the energy and character of the frontier orbitals of the cations  $[\text{Cu}(\text{L})_2(\text{NCO})]^+$ ,  $[\text{Cu}(\text{L})_2(\text{NCS})]^+$  and  $[\text{Cu}(\text{L})_2(\text{NCSe})]^+$  are shown in Figs. 7–9, respectively. For all complexes the highest the MO presents significant ligand character. It is predominately of  $-\text{NCX}$  ligand (>70%) with some contributions from the *d* orbitals of the copper (II) ion (~1–8%). The LUMO

**Table 6**Selected theoretical bond distances and angles for Cu–NCS and Cu–SCN isomers of  $[\text{Cu}(\text{L})_2(\text{NCS})]\text{ClO}_4$  calculated at B3LYP/6-311G level of theory.

Bond distances (Å)	Cu–NCS		Cu–SCN		Bond angles (°)	Cu–NCS		Cu–SCN	
N(1)–Cu(1)	1.984	–	–	–	N(4)–Cu(1)–N(3)	168.3	–	166.4	–
S(1)–Cu(1)	–	2.494	–	–	N(4)–Cu(1)–N(2)	96.4	–	92.9	–
N(2)–Cu(1)	2.150	2.235	–	–	N(3)–Cu(1)–N(2)	83.3	–	82.7	–
N(3)–Cu(1)	2.160	2.160	–	–	N(1)–Cu(1)–N(5)	97.9	–	–	–
N(4)–Cu(1)	2.128	2.124	–	–	N(4)–Cu(1)–N(5)	80.8	–	81.8	–
N(5)–Cu(1)	2.489	2.414	–	–	N(5)–Cu(1)–N(3)	110.9	–	111.5	–
C(1)–N(1)	1.201	1.182	–	–	N(2)–Cu(1)–N(5)	95.5	–	70.0	–
C(1)–S(1)	1.661	1.729	–	–	C(1)–N(1)–Cu(1)	145.0	–	–	–
Bond angles (°)					N(1)–C(1)–S(1)	179.3	–	179.4	–
N(1)–Cu(1)–N(4)	87.6	–	–	–	C(1)–S(1)–Cu(1)	–	–	109.2	–
N(1)–Cu(1)–N(3)	90.1	–	–	–					
N(1)–Cu(1)–N(2)	166.4	–	–	–					

**Table 7**Selected theoretical bond distances and angles for Cu–NCSe and Cu–SeCN isomers of  $[\text{Cu}(\text{L})_2(\text{NCSe})]\text{ClO}_4$  calculated at B3LYP/6-311G level of theory.

Bond distances (Å)	Cu–NCSe		Cu–SeCN		Bond angles (°)	Cu–NCSe		Cu–SeCN	
N(1)–Cu(1)	1.994	–	–	–	N(4)–Cu(1)–N(3)	168.2	–	167.8	–
Se(1)–Cu(1)	–	2.616	–	–	N(4)–Cu(1)–N(2)	96.6	–	92.7	–
N(2)–Cu(1)	2.155	2.256	–	–	N(3)–Cu(1)–N(2)	83.3	–	82.8	–
N(3)–Cu(1)	2.169	2.150	–	–	N(1)–Cu(1)–N(5)	96.2	–	–	–
N(4)–Cu(1)	2.136	2.119	–	–	N(4)–Cu(1)–N(5)	80.9	–	81.6	–
N(5)–Cu(1)	2.479	2.436	–	–	N(5)–Cu(1)–N(3)	110.9	–	110.1	–
C(1)–N(1)	1.120	1.181	–	–	N(2)–Cu(1)–N(5)	96.3	–	96.3	–
C(1)–Se(1)	1.789	1.851	–	–	N(1)–Cu(1)–N(2)	165.4	–	–	–
Bond angles (°)					C(1)–N(1)–Cu(1)	147.6	–	–	–
N(1)–Cu(1)–N(4)	87.4	–	–	–	N(1)–C(1)–Se(1)	180.0	–	179.7	–
N(1)–Cu(1)–N(3)	90.0	–	–	–	C(1)–Se(1)–Cu(1)	–	–	106.9	–
N(1)–Cu(1)–N(2)	165.4	–	–	–					

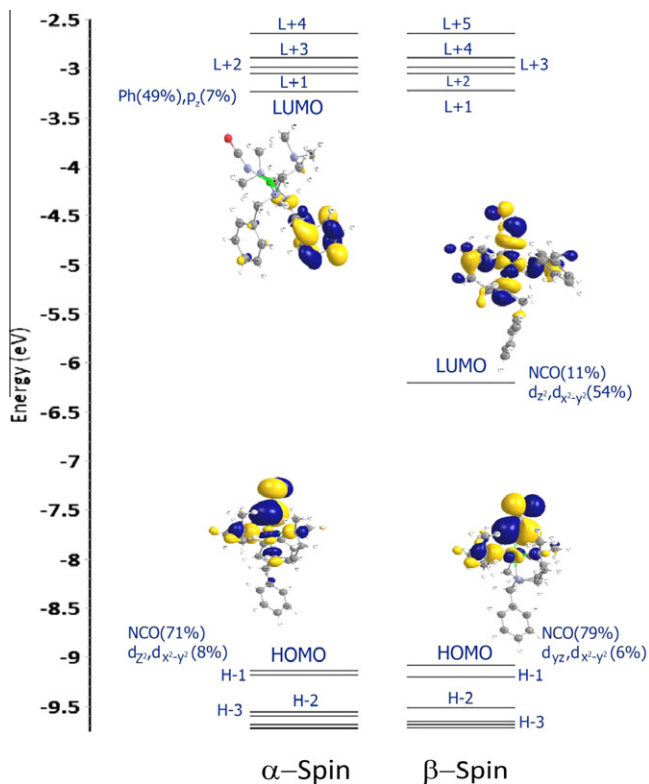
**Fig. 6.** Calculated molecular structures of  $[\text{Cu}(\text{L})_2(\text{NCS})]^+$ , and  $[\text{Cu}(\text{L})_2(\text{NCSe})]^+$ .

orbitals of the complexes are composed of the copper *d*-orbitals (~50%), –NCX and chelated ligands, L.

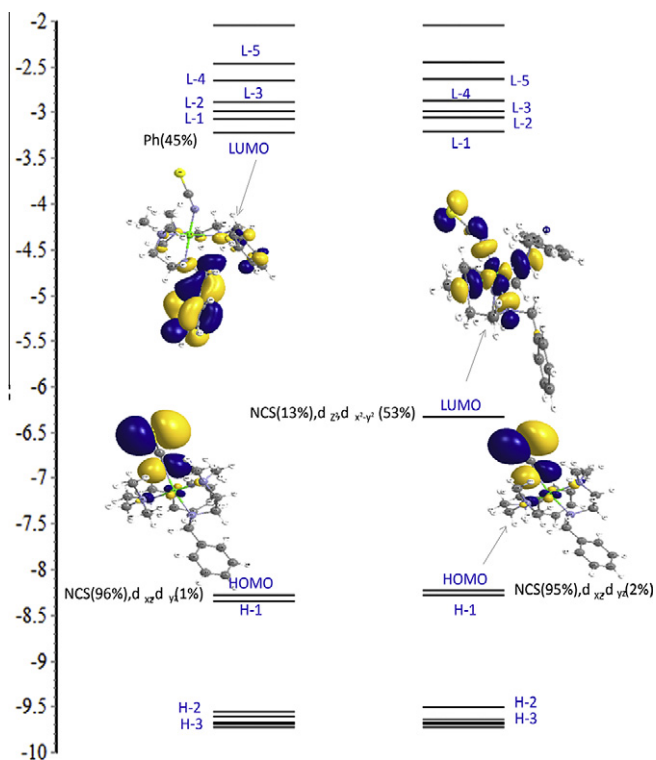
### 3.5. Solvatochromism

The complexes **1** and **2** are fairly soluble in various organic solvents and demonstrate distinctive solvatochromism. Solvatochromism is the ability of a compound to change color due to a

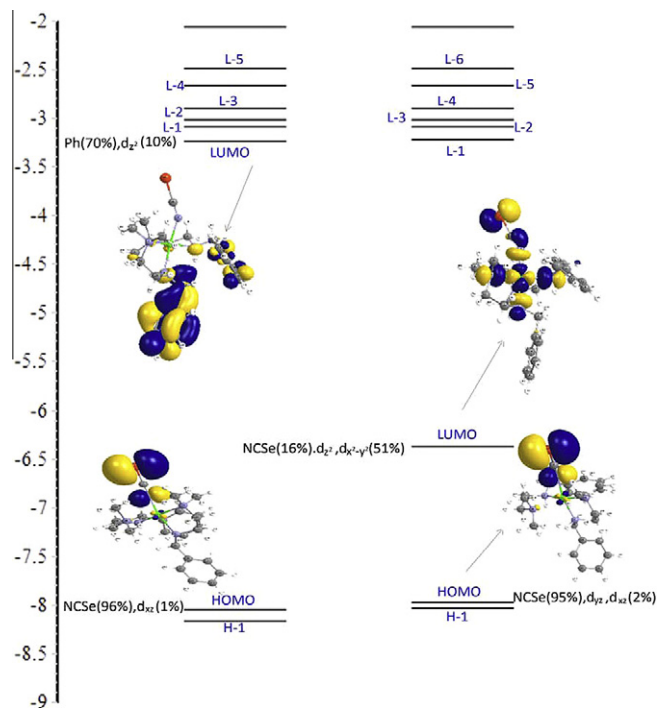
change in solvent polarity. The origin of the color changes in these compounds are attributed to the shift in the *d*–*d* transition of the copper (II) ions as results of solvent–solute interactions. The spectra in all solvent have nearly the same pattern of octahedral complexes with almost equal intensities. The visible spectral changes of these complexes in the selected solvents are illustrated in Fig. 10. The positions of the  $\nu_{\text{max}}$  values of the complexes along with the molar absorptivities are collected in Table 8.



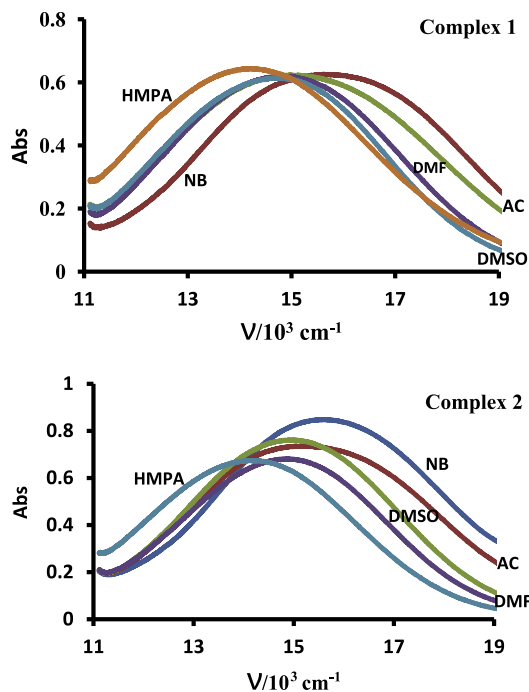
**Fig. 7.** The energy (eV), character and some contours of the molecular orbitals of  $[\text{Cu}(\text{L})_2(\text{NCO})]^+$ . Positive values of the orbital contour are represented in yellow and negative values in blue.



**Fig. 8.** The energy (eV), character and some contours of the molecular orbitals of  $[\text{Cu}(\text{L})_2(\text{NCS})]^+$ . Positive values of the orbital contour are represented in yellow and negative values in blue.



**Fig. 9.** The energy (eV), character and some contours of the molecular orbitals of  $[\text{Cu}(\text{L})_2(\text{NCSe})]^+$ . Positive values of the orbital contour are represented in yellow and negative values in blue.

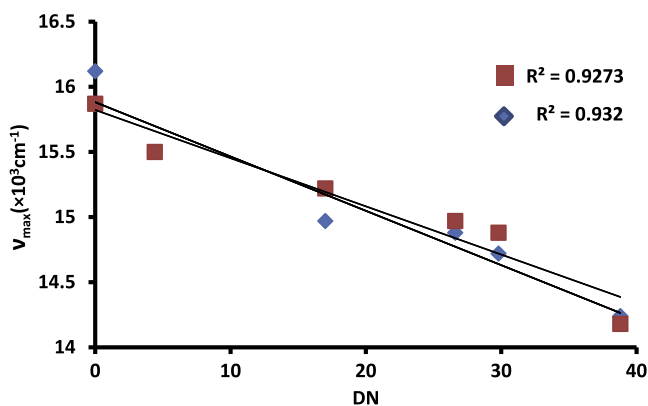


**Fig. 10.** Absorption spectra of complexes 1 and 2 in selected solvents.

The broad structureless visible band is related to the transition of the electron from the lower energy orbitals to the hole in  $d_{x^2-y^2}$  orbital of the copper (II) ion ( $d^9$ ). The electronic absorption spectra of the complexes were measured in solution state in some organic solvents with different donor number (DN). The donor number expresses a measure of coordinating ability of solvent on the

**Table 8**Electronic absorption maxima of the complexes in various solvents:  $\nu_{\max}/10^3 \text{ cm}^{-1}$  ( $\epsilon/M^{-1} \text{ cm}^{-1}$ ).

Solvent	DCM	BN	AC	DMF	DMSO	HMPA
DN	0.0	4.4	17.0	26.6	29.8	38.8
Complex 1	16.12 (122)	15.5 (120)	14.97 (123)	14.88 (100)	14.72 (124)	14.24 (129)
Complex 2	15.87 (170)	15.5 (150)	15.22 (139)	14.97 (136)	14.88 (153)	14.18 (135)

**Fig. 11.** Dependence of the  $\nu_{\max}$  values of compounds **1** and **2** on the solvent donor number values.

standard of that of dichloromethane (DCM) or dichloroethane (DCE) [54]. The values of DN of the solvents used are as follows: DCM and DCE = 0.0; MeNO<sub>2</sub> = 2.7; acetone = 17.0; MeOH = 19.0; THF = 20.0 DMF = 26.6; DMSO = 29.8; HMPA = 38.8.

In solution the d–d band of all complexes moves to the red with the increase of the DN of the solvent (Table 7 and Fig. 10). As the results illustrate, the energy change on the absorption spectra of the compounds is as large as 1690–1880 cm<sup>-1</sup> over the solvents studied. The greatest solvatochromic effect is displayed by complex **1** (1880 cm<sup>-1</sup>). Assuming that the approach of the solvent occurs along the empty z axis, the solvent molecule is repelled by the two electrons in the d<sub>z<sup>2</sup></sub> orbital of the copper (II) and only the more basic species can force their way into form relatively strong bonds. Upon coordination, they exert a z component field proportional to their position in the spectrochemical series. Thus, while solvents of low basicity (low donor number) have less effect in the band maxima, others that are considerably more basic induce large red shifts.

Regression analysis of the band maxima of the complexes against donor number of solvents is shown in Fig. 11 and indicates good correlations and also confirms the solvatochromic behavior of the complexes. A linear correlation of the  $\nu_{\max}$  values with the solvent donor number (DN) yields the following expression. Thus the solvatochromic behavior the complex can be studied quantitatively.

$$\text{Complex 1: } \nu_{\max}/10^3 = -0.0417\text{DN}_{\text{solv}} + 15.822, R = 0.963$$

$$\text{Complex 2: } \nu_{\max}/10^3 = -0.037\text{DN}_{\text{solv}} + 15.822, R = 0.969$$

#### 4. Conclusion

Three mononuclear copper (II) pseudohalide complexes were synthesized and characterized. X-ray structure determination of [Cu(L)<sub>2</sub>(NCO)]ClO<sub>4</sub> showed a square pyramidal structure around the metal center. The scope of these studies was extended to include a series of XCN<sup>-</sup>-terminal mononuclear complexes. A similar coupling scheme was used to synthesize the copper(II) analogue, yielding the cationic complexes. All the copper complexes are

isostructural as elucidated by spectroscopic and X-ray diffraction analysis. DFT calculations show that Cu–NCX is more stable than Cu–XCN by 43.71 kJ mol<sup>-1</sup> for complex **1**, 49.8 kJ mol<sup>-1</sup> for complex **2** and 39.9 kJ mol<sup>-1</sup> for complex **3**. Complexes **1** and **2** showed solvatochromism. The complexes confirmed a good correlation between their d–d absorption maxima in solution and the donor number of the solvent used (positive solvatochromism) due to coordination of solvent molecules with different donor power to the axial site of the copper (II) ion that results in changing the geometry of the complexes from square pyramid to the octahedron.

#### Acknowledgment

We are grateful for the financial support of university of Mazandaran of the Islamic Republic of Iran.

#### Appendix A. Supplementary material

CCDC 901582 contains the supplementary crystallographic data for this paper. These data can be obtained free of charge via [www.ccdc.cam.ac.uk/conts/retrieving.html](http://www.ccdc.cam.ac.uk/conts/retrieving.html) or from the Cambridge Crystallographic Data Centre, 12, Union Road, Cambridge CB2 1EZ, UK; fax: (+44) 1223 336033; or e-mail: [deposit@ccdc.cam.ac.uk](mailto:deposit@ccdc.cam.ac.uk). Supplementary data associated with this article can be found, in the online version, at <http://dx.doi.org/10.1016/j.poly.2012.12.009>.

#### References

- [1] C. Buda, A.B. Kazi, A. Dinescu, T.R. Cundari, J. Chem. Inf. Model. 45 (2005) 965.
- [2] A.R. Khan, S.M. Socol, D.W. Meek, R. Yasmeen, Inorg. Chim. Acta 234 (1995) 109.
- [3] S. Chowdhury, N. Koshino, A. Canlier, K. Mizuoka, Y. Ikeda, Inorg. Chim. Acta 359 (2006) 2472.
- [4] J.S. Gancheff, Á. Acosta, D. Armentano, G. De Munno, R. Chiozzzone, R. González, Inorg. Chim. Acta 387 (2012) 314.
- [5] R. González, N. Barboza, R. Chiozzzone, C. Kremer, D. Armentano, G. De Munno, J. Faus, Inorg. Chim. Acta 361 (2008) 2715.
- [6] T.P. Brewster, W. Ding, N.D. Schley, N. Hazari, V.S. Batista, R.H. Crabtree, Inorg. Chem. 50 (2011) (1946) 11938.
- [7] M. Cusumano, G. Guglielmo, P. Marricchi, V. Ricevuto, Inorg. Chim. Acta 30 (1978) 29.
- [8] H. Ohtsu, N. Oka, T. Yamaguchi, Inorg. Chim. Acta 383 (2012) 1.
- [9] L.J. Cavichio, T. Hasegawa, F.S. Nunes, Spectrochim. Acta, Part A 64 (2006) 161.
- [10] L.K. Das, A. Biswas, A. Frontera, A. Ghosh, Polyhedron <http://dx.doi.org/10.1016/j.poly.2012.04.029>, 2012.
- [11] B. Machura, A. Switlicka, M. Penkala, Polyhedron 45 (2012) 221.
- [12] J. Lu, H.-T. Liu, D.-Q. Wang, X.-X. Zhang, J. Mol. Struct. 938 (2009) 299.
- [13] M. Kabešova, R. Boca, M. Melnik, D. Valigura, M. Dunaj-Jurco, Coord. Chem. Rev. 140 (1995) 115.
- [14] M. Du, Ch.-Peng Li, X.-J. Zhao, Cryst. Eng. Commun. 8 (2006) 552.
- [15] J.Y. Lu, Coord. Chem. Rev. 246 (2003) 327.
- [16] F.H. Allen, Acta Crystallogr., Sect. B 58 (2002) 380.
- [17] B.J. Hathaway, in: G. Wilkinson, R.D. Gillard, J.A. McCleverty (Eds.), Comprehensive Coordination Chemistry, vol. 5, Pergamon Press, Oxford, England, 1987, p. 533.
- [18] P. Coppens, I. Novozhilova, A. Kovalevsky, Chem. Rev. 102 (2002) 861.
- [19] A.Y. Kovalevsky, K.A. Bagley, P. Coppens, J. Am. Chem. Soc. 124 (2002) 9241.
- [20] G.K. Chaitanya, K. Bhanuprakash, M.K. Nazeeruddin, M. Grätzel, P.Y. Reddy, Inorg. Chem. 45 (2006) 7600.
- [21] M. Calligaris, Coord. Chem. Rev. 248 (2004) 351.
- [22] I. Ciofini, C.A. Daul, C. Adamo, J. Phys. Chem. A 107 (2003) 11182.
- [23] N.S. Panina, M. Calligaris, Inorg. Chim. Acta 334 (2002) 165.
- [24] M. Stener, M. Calligaris, J. Mol. Struct. (THEOCHEM) 497 (2000) 91.
- [25] H. Golchoubian, E. Rezaee, J. Mol. Struct. 929 (2009) 154.

- [26] Stoe & Cie, X-AREA (version 1.26), Stoe & Cie GmbH, Darmstadt, Germany, 2007.
- [27] G.M. Sheldrick, SADABS, University of Göttingen, Germany.
- [28] G.M. Sheldrick, Acta Crystallogr., Sect. A 64 (2008) 112.
- [29] Stoe & Cie, X-RED (version 1.28b), Stoe & Cie GmbH, Darmstadt, Germany, 2005.
- [30] G.M. Sheldrick, Acta Crystallogr., Sect. A 64 (2008) 112.
- [31] A.L. Spek, Acta Crystallogr., Sect. D 65 (2009) 148.
- [32] K. Brandenburg, DIAMOND, Crystal Impact GbR, Bonn, Germany, 2001.
- [33] C.F. Macrae, I.J. Bruno, J.A. Chisholm, P.R. Edgington, P. McCabe, E. Pidcock, L. Rodriguez-Monge, R. Taylor, J. van de Streek, P.A. Wood, J. Appl. Crystallogr. 41 (2008) 466.
- [34] GAUSSIAN 09, Revision A.02, M.J. Frisch, G.W. Trucks, H.B. Schlegel, G.E. Scuseria, M.A. Robb, J.R. Cheeseman, G. Scalmani, V. Barone, B. Mennucci, G.A. Petersson, H. Nakatsuji, M. Caricato, X. Li, H.P. Hratchian, A.F. Izmaylov, J. Bloino, G. Zheng, J.L. Sonnenberg, M. Hada, M. Ehara, K. Toyota, R. Fukuda, J. Hasegawa, M. Ishida, T. Nakajima, Y. Honda, O. Kitao, H. Nakai, T. Vreven, J.A. Montgomery, Jr., J.E. Peralta, F. Ogliaro, M. Bearpark, J.J. Heyd, E. Brothers, K.N. Kudin, V.N. Staroverov, R. Kobayashi, J. Normand, K. Raghavachari, A. Rendell, J.C. Burant, S.S. Iyengar, J. Tomasi, M. Cossi, N. Rega, J. M. Millam, M. Klene, J.E. Knox, J.B. Cross, V. Bakken, C. Adamo, J. Jaramillo, R. Gomperts, R.E. Stratmann, O. Yazyev, A.J. Austin, R. Cammi, C. Pomelli, J.W. Ochterski, R.L. Martin, K. Morokuma, V.G. Zakrzewski, G.A. Voth, P. Salvador, J.J. Dannenberg, S. Dapprich, A.D. Daniels, O. Farkas, J.B. Foresman, J.V. Ortiz, J. Cioslowski, D.J. Fox, Gaussian, Inc., Wallingford, CT, 2009.
- [35] A.D. Becke, J. Chem. Phys. 98 (1993) 5648.
- [36] C. Lee, W. Yang, R.G. Parr, Phys. Rev. B37 (1988) 785.
- [37] P.J. Hay, W.R. Wadt, J. Chem. Phys. 82 (1985) 270 (and also 299).
- [38] W.R. Wadt, P.J. Hay, J. Chem. Phys. 82 (1985) 284.
- [39] P.J. Hay, W.R. Wadt, J. Chem. Phys. 82 (1985) 299.
- [40] M.G.B. Drew, D. Das, S. De, D. Datta, Inorg. Chim. Acta 362 (2009) 1501.
- [41] F.A. Mautner, R. Vicenta, S.S. Massoud, Polyhedron 25 (2006) 1673.
- [42] C. Tsiamis, M. Themeli, Inorg. Chim. Acta 206 (1993) 105.
- [43] H. Chowdhury, S.H. Rahaman, R. Ghosh, S.K. Sarkar, H.K. Fun, B.K. Ghosh, J. Mol. Struct. 826 (2007) 170.
- [44] S. Banerjee, M.G.B. Drew, C.Z. Lue, J. Tercero, C. Diaz, A. Ghosh, Eur. J. Inorg. Chem. (2005) 2376.
- [45] C. Diaz, J. Ribas, M.S. El Fallah, X. Solans, M. Font-Bardia, Inorg. Chim. Acta 312 (2001) 1.
- [46] S. Banerjee, M.G.B. Drew, C.Z. Lue, J. Tercero, C. Diaz, A. Ghosh, Eur. J. Inorg. Chem. (2005) 237.
- [47] S. Massoud, F. Mautner, Inorg. Chim. Acta 358 (2005) 3334.
- [48] Z.D. Georgousis, P.C. Christidis, D. Hadjipavlou-Litinac, C.A. Bolos, J. Mol. Struct. 837 (2007) 30.
- [49] W.J. Geary, Coord. Chem. Rev. 7 (1971) 81.
- [50] A.W. Addison, T.N. Rao, J. Chem. Soc., Dalton Trans. 1 (1984) 1349.
- [51] H. Asadi, H. Golchoubian, R.J. Welter, Mol. Struct. 779 (2005) 30.
- [52] H. Golchoubian, G. Moayyedi, G. Bruno, H.A. Rudbari, Polyhedron 30 (2011) 1027.
- [53] H. Golchoubian, R.Z. Zarabi, Polyhedron 28 (2009) 3685.
- [54] V. Gutmann, Coordination Chemistry in Non-aqueous Solutions, Springer, Vienna, 1968.